Porphyrin Derivatives Mediated Sonodynamic Therapy on Malignant Gliomas in Vitro

Shogo ENDO[1)], Nobuki KUDO[2)], Shigeru YAMAGUCHI[1)], Koki SUMIYOSHI[2)], Hiroaki MOTEGI[1)], Hiroyuki KOBAYASHI[1)], Shunsuke TERASAKA[1)], Kiyohiro HOUKIN[1)]

1. Department of Neurosurgery, Graduate School of Medicine, Hokkaido University
2. Laboratory of Biological Engineering, Graduate School of Information Science and Technology, Hokkaido University

Correspondence:

Hiroyuki Kobayashi, MD

Department of Neurosurgery, Graduate School of Medicine, Hokkaido University, North 15 West 7, Kita-ku, Sapporo, 060-8638, Japan

Tel: +81-11-706-5987

Fax: +81-11-708-7737

E-mail: hiro-ko@med.hokudai.ac.jp

ABSTRACT

Due to its highly infiltrative property, malignant glioma is a cancer of poor prognosis despite multidisciplinary treatment strategies, such as aggressive surgery and chemoradiotherapy, unveiling a need for new therapeutic approaches to control migrated tumor cells. In our study, we investigated the efficacy of sonodynamic therapy (SDT) using porphyrin derivatives involving 5-aminolevulinic acid, protoporphyrin IX, and talaporfin sodium as sonosensitizers on glioma cells, in vitro. These substances have been known to accumulate in glioma cells and are expected to have cytotoxic effects by sonication. Our study demonstrated that the cytotoxicity of sonication on glioma cells was enhanced by each sonosensitizer and the efficacy of the SDT may depend on the degree of intracellular accumulation of sonosensitizer. Also, induction of apoptosis was suggested to be a major mechanism of cell death. Though further investigations will be necessary, our preliminary result showed a potential of SDT with sonosensitizers for glioma treatment.

KEYWORDS: 5-aminolevulinic acid, in vitro, malignant glioma, porphyrin derivatives, protoporphyrin IX, sonodynamic therapy, talaporfin sodium, ultrasound

INTRODUCTION

Gliomas account for approximately 20 % of primary brain tumors in adults (Nakamura et al. 2011). Regarding the malignant subtype of glioma, prognosis is very poor. Despite intensive therapy, the actual 2-year survival rate is only 33.9 % (Chinot et al. 2014; Gilbert et al. 2014). Though novel therapeutic trials have been recently carried out, patients' survival has not been improved remarkably. Thus, it is necessary to develop a different approach to treatment, enhancing conventional therapy. At present, the standard treatment for malignant gliomas is maximal safe resection combined with chemoradiation. Removal of the tumor is still the most important role in a therapeutic strategy, but the boundary of the tumor is often unclear because glioma cells infiltrate into adjacent normal brain tissue. Actually, 90 % of tumors relapse within 2 cm of the primary site despite the use of chemoradiotherapy after gross total resection (Wilson 1992). These results suggest a key of successful treatment is to control these infiltrative tumor cells.

Photodynamic therapy (PDT) is one of the expected treatments (Muragaki et al. 2013). The mechanism of this therapy is that photochemically activated photosensitizers

34 generate reactive oxygen species (ROS), such as singlet oxygen and free radicals, which
35 lead to oxidative damage of target tumor cells. Among various photosensitizers,
36 porphyrin derivatives have been utilized in PDT for gliomas because these substances
37 are selectively accumulated in glioma cells, and they have been already applied for
38 clinical use in PDT and intraoperative fluorescence diagnosis (Stylli et al. 2006a; Stylli
39 et al. 2006b). Particularly, 5-Aminolevulinic acid (ALA) is widely used for
40 intraoperative fluorescence diagnosis. ALA, which is a natural amino acid, is the first
41 compound of the porphyrin biosynthetic pathway. In this pathway, protoporphyrin IX
42 (PpIX) is synthesized from ALA in mitochondria, and PpIX is suggested to be retained
43 in tumor cells when administrating exogenous ALA excessively. This is thought to be
44 due to metabolic dysfunction of PpIX in malignant tumor cell (Ishizuka et al. 2011).
45 Accumulated PpIX in a tumor cell acts as a strong photosensitizer. Furthermore,
46 talaporfin sodium (TS) is a second-generation photosensitizer that has recently been
47 approved in Japan for PDT to treat primary malignant brain tumors (Muragaki et al.
48 2013). Although PDT is an attractive treatment in glioma therapy, there is a great
49 problem of penetration depth of the light in brain tissue. To overcome this issue,

ultrasound has been expected as alternative energy source to excite the photosensitizers. Rosenthal et al. have shown that various photosensitizers are excited by ultrasound as well (Rosenthal et al. 2004).

The aim of this study is to investigate the anti-tumor effects of SDT with porphyrin derivatives such as ALA, PpIX, and TS for gliomas in vitro.

MATERIAL AND METHODS

Reagents

ALA was purchased from COSMO BIO Co., Ltd (Koto, Tokyo, Japan). PpIX, Hoechst 33342 (bis Benzimide H 33342 trihydrochloride), and Propidium iodide (PI) were purchased from Sigma-Aldrich (St. Louis, MO, USA). TS was purchased from Meiji seika, Ltd. (Chuo, Tokyo, Japan). Calcein AM/Ethidium homodimer (EthD-1) costaining kit (Live/Dead Viability/Cytotoxicity Assay Kit®) was purchased from Life Technologies (Minato, Tokyo, Japan). Annexin V-FLUOS Staining Kit was purchased from Roche Applied Science (Minato, Tokyo, Japan).

66 *Cell culture*

67 Rat glioma cell line C6 and human glioblastoma cell line U87MG were obtained from
68 the American Type Culture Collection (Manassas, VA, USA). Cells were maintained as
69 monolayers in Dulbecco's Modified Eagle Medium (DMEM; Sigma-Aldrich, St. Louis,
70 MO, USA) supplemented with 10 % heat-inactivated fetal bovine serum (FBS; Life
71 Technologies, Minato, Tokyo, Japan), 100 U/mL of penicillin G, and 100 μg/mL of
72 streptomycin (Sigma-Aldrich, St. Louis, MO, USA) at 37 ℃ in a humidified incubator
73 with 5 % CO_2 in air atmosphere. Unless stated otherwise, the conditions of the
74 incubation were as described above. Cells in the exponential growth phase after more
75 than 5 passages were used for all of the following experiments.

76

77 *Ultrasound exposure apparatus*

78 The ultrasound exposure apparatus was arranged as shown in Fig. 1. A
79 laboratory-assembled planar circular transducer (30 mm in diameter) with air backing
80 was submerged in a water bath ($0.4\times0.2\times0.1$ m^3) filled with degassed water to avoid
81 attenuation of ultrasound wave, and facing upward with its acoustic surface parallel to

82 the water surface. A function generator (AFG3022, Tektronix, Minato, Tokyo, Japan)
83 was used to generate burst pulses of 1 MHz in center frequency and 100 Hz in pulse
84 repetition frequency. Burst pulses of 50 % in duty cycle contain 5,000 cycles in each
85 burst. The transducer was driven by the signal amplified using a power amplifier
86 (UOD-WB-1000, Tokin, Sendai, Miyagi, Japan). The spatial-average-temporal-average
87 intensity (I_{SATA}) of 0.16 W/cm^2 was used for all experiments, which was determined by
88 pressure calibration using an apparatus utilized for our previous study. (Yamaguchi et al.
89 2011) The calibration was carried out in a free water condition using a Polyvinylidene
90 difluoride membrane hydrophone (MHB-500, Onda, Sunnyvale, CA, USA). During
91 ultrasound exposure, the flat bottom of the well plate (MULTIWELL^{TM} 6 well, BD
92 FALCON$^{®}$, Bedford, MA, USA) was placed 5 mm from the surface of the transducer.
93 In this condition, the estimation of I_{SATA} that cells actually received is technically
94 difficult because strong reflections at the water surface generate a standing wave field
95 inside the well. An acoustic absorbing rubber plate is frequently used to prevent the
96 reflection by placing it on the water surface. However, it was not utilized in the
97 experiments to minimize disturbance in culture condition and the possibility of

98 contamination because cell incubation should be continued for up to 24 hours after the
99 sonication. The wells measured 35 mm in diameter, 18 mm in depth, and were 1.62 mm
100 thick. Furthermore, the height (volume) of solution in each well was stringently unified
101 at 1.3 mm (4 mL/well) because the sound pressure transferred to the cells from the
102 standing waves varied depending on the fluid surface height (data not shown). The
103 water temperature in the bath was held at 37 ℃ to eliminate the temperature elevation
104 of treated cells.
105
106 *SDT treatment protocols*
107 Cells were randomly divided into four treatment groups: control, sonosensitizer
108 exposure, ultrasound exposure, and SDT (ultrasound exposure plus sonosensitizer
109 exposure). Upon reaching 70 % confluence, cells were washed with phosphate-buffered
110 saline (PBS; Nacalai tesque, Nakagyo, Kyoto, Japan) and collected using 0.05 % trypsin
111 with 0.53 mM ethylenediaminetetraacetic acid. Approximately 3.0×10^5 cells/well were
112 dispersed into the wells of each plate and subsequently incubated for 24 hours.

ALA and TS were stored at 4 ℃ in the dark, and dissolved in DMEM without phenol-red (Sigma-Aldrich, St. Louis, MO, USA) to a final concentration of 200 and 30 μg/mL respectively. PpIX was dissolved in dimethyl sulfoxide (Sigma-Aldrich, St. Louis, MO, USA) at a concentration of 0.005 g/mL and subsequently stored at -20 ℃ in the dark, and also dissolved in DMEM without phenol-red to a final concentration of 1.0 μg/mL. For the sonosensitizer and the SDT groups, the culture medium was replaced with an equivalent volume of sonosensitizer solution and incubated thereafter for 4 hours. For the other groups, the culture medium was replaced with fresh DMEM without sonosensitizer solution and phenol-red and subsequently incubated. Consecutively each well in the ultrasound and the SDT groups was subjected to ultrasound treatment at 1.0 MHz and 0.16 W/cm^2 for 60 seconds respectively.

Fluorescence intensity per cell after co-incubation with each sonosensitizer

The fluorescence intensity per cell after co-incubation with each sonosensitizer was analyzed by flow cytometry to verify differences in the uptake of the sonosensitizer in different cell lines. Following co-incubation with each sonosensitizer, cells were

129 harvested by trypsin and analyzed by a flow cytometer (Attune® Acoustic Focusing
130 Cytometer, Life Technologies, Minato, Tokyo, Japan) using excitation and emission
131 wavelengths of 488 and 690/50 nm, respectively.
132
133 *Cytotoxicity of SDT*
134 Following ultrasound exposure, cells were re-incubated for 24 hours. A Calcein
135 AM/EthD-1 costaining kit was used with Hoechst 33342 following incubation to assess
136 cell viability. After washing the cells with 1 mL of PBS, 100 μL of PBS containing 2
137 μM of Calcein AM and 4 μM of EthD-1, and 0.2 μL of Hoechst 33342 were added to
138 each well and the cells were incubated for 30 minutes at room temperature in the dark.
139 Cells were observed using a fluorescent microscope (IX71, U-LH100HGAPO,
140 OLYMPUS, Shinjuku, Tokyo, Japan). The polyanionic dye Calcein AM is well retained
141 within live cells, producing an intense uniform green fluorescence. EthD-1 enters cells
142 with damaged membranes and binds to nucleic acids, thereby producing a bright red
143 fluorescence in dead cells. Hoechst 33342 is a popular cell-permeation nuclear
144 counterstain that emits blue fluorescence when bound to double-stranded

deoxyribonucleic acid (DNA), regardless of cell survival. The average numbers of green, red, and blue fluorescent cells were calculated in five random microscopic fields with at least 1000 cells/field for each treatment group. Experiments were repeated independently three times. Notably, exfoliated floating cells at 24 hours after treatment were defined as dead.

The number of dead cells was calculated as [*number of Hoechst 33342 positive cells in control group － number of Hoechst 33342 positive cells in each treatment group*].

Thus, compensated dead cells were estimated as [*number of EthD-1 positive cells in each treatment group ＋ number of dead cells in each treatment group*].

The survival rate (%) of the tumor cells was calculated as [*100 − number of compensated dead cells in each treatment group / number of Hoechst 33342 positive cells in control group × 100*].

Mechanism of ALA mediated SDT cytotoxicity on C6 cells

Treated C6 cells were stained with Annexin V-FLUOS and PI to assess the cell damage mechanism following re-incubation for 6 hours. After washing once with 1 mL

161 of PBS, 100 μL of the incubation buffer (10 mM Hepes、pH7.4、140 mM NaCl、5 mM
162 $CaCl_2$) containing 2 μL of Annexin V-FITC and 2 μL of PI (50 μg/mL) was added to
163 each well. Cells were then incubated for 15 minutes at room temperature in the dark.
164 The cells were trypsinized, and then analyzed using a flow cytometer with an excitation
165 wavelength of 488 nm and emission wavelength of 530/30 nm for Annexin V-FLUOS
166 and 574/26 nm for PI respectively. Phosphatidyl serine (PS) is located on the
167 cytoplasmic surface of the cell membrane in live cells; however, it is translocated from
168 the inner to the outer leaflet of the plasma membrane in the acute phase of apoptosis,
169 while Annexin V-FLUOS has a high affinity for PS exposed on the outer leaflet and
170 produces green fluorescence. PI is impermeant to live and apoptotic cells; however, it
171 binds tightly to the nucleic acids in dead cells, producing red fluorescence.
172
173 *Statistical analysis*
174 Experimental data was analyzed statistically with Statcel 3 software (OMS publishing
175 Inc, Tokorozawa, Saitama, Japan). All values were presented as means ± standard
176 deviation of triplicate experiments. The comparisons among these groups were assessed

177 by one-way analysis of variance (ANOVA) followed by Tukey-Kramer test and p

178 values < 0.05 were considered to be statistically significant.

179

180 **RESULTS**

181 *Cytotoxicity of SDT with each sonosensitizer on C6 cells*

182 The survival rate was evaluated by counting the number of live and dead cells with a

183 fluorescent microscope. The number of exfoliated cells was prominent in the SDT

184 group (Fig. 2). The cytotoxicity of the ultrasound was enhanced by each sonosensitizer

185 on C6 cells, while neither each sonosensitizer alone nor ultrasound alone caused any

186 cytotoxicity. The survival rate of C6 cells treated by ALA mediated SDT decreased

187 from 85.1±6.8 % to 69.1±10.8 % (Fig. 3a), as well as for PpIX mediated SDT (from

188 100.0±11.7 % to 78.9±1.0 %, Fig. 3b) and for TS mediated SDT (from 100.0±11.7 % to

189 59.8±8.1 %, Fig. 3c). Furthermore, for all sonosensitizers, the survival rates of the SDT

190 groups were lower than those from any of the other groups.

191

192 *Mechanism of ALA mediated SDT cytotoxicity on C6 cells*

193 Flow cytometry analysis demonstrated marked changes in the cell profile following
194 ultrasound exposure on C6 cells (Fig. 4). The results of flow cytometry analysis were
195 the following: cells in the lower-left quadrant (Annexin-V-/PI-) represent living cells,
196 those in the lower-right quadrant (Annexin-V+/PI-) represent early apoptotic cells, and
197 those in the upper-right quadrant (Annexin-V+/PI+) represent late apoptotic cells or
198 necrotic cells. The early apoptotic cell rate in both ultrasound alone and SDT group
199 were more than twice as high as that in the other groups, respectively (ultrasound alone
200 group: Figure 4c 14.2 % and SDT group: Figure 4d 20.4 % vs. Control group: Figure 4a
201 5.1 % and ALA alone group: Figure 4d 1.5 %). In addition, late apoptotic and necrotic
202 cell rates in the SDT group were the highest among all groups (Figure 4d).
203
204 *Comparison of the cytotoxicity of SDT between C6 and U87MG cells*
205 The cytotoxic effect of SDT on U87MG cells (Figure 3d-f) was smaller than that on
206 C6 cells despite the fact that it was applied under the same conditions as for C6 in each
207 sonosensitizer administered (Figure 3a-c). Figure 5 shows the results of the difference in
208 uptake of sonosensitizer between these two cell lines in flow cytometry analysis. For

209 either sonosensitizer, the fluorescence intensity per cell of U87MG cells (Figure 5d-f)
210 was lower than that of C6 cells (Figure 5a-c).
211
212 **DISCUSSION**
213 Although various therapeutic strategies for malignant gliomas have been tried
214 clinically, satisfactory results have not been obtained yet (Chinot et al. 2014; Miyatake
215 et al. 2014; Thomas et al. 2014). Japanese national survey reported that 1-, 2-, and
216 3-years survival rates of patients with malignant gliomas was approximately 60.3 %,
217 25.4 %, 15.9 %, respectively (Report of brain tumor registry of Japan (2001-2004) 13th
218 edition 2014). Therefore, new methods of treatment should be developed as a
219 breakthrough of this situation.
220 Since the 80's, PDT has been explored as a novel option to treat malignant gliomas
221 because this therapy is of low toxicity for normal brain tissue by tumor-selectivity of
222 photosensitizers (Stylli et al. 2006a; Stylli et al. 2006b). However, the most important
223 problem of PDT is the limited penetration depth of the light in brain tissue. It was
224 reported that the effective depth of laser beam penetration in brain tissue is

225 approximately 0.75–1.5 cm (Muragaki et al. 2013). This issue was recognized from the
226 beginning of the development of PDT. To overcome this issue, basic experiments were
227 conducted to confirm whether ultrasound could be used as an alternative to the light for
228 excitation of photosensitizers (Rosenthal et al. 2004; Chen et al. 2014). Further studies
229 have shown the cytotoxic effect of SDT, which was combined ultrasound and
230 conventional photosensitizers, for various cancers (Canaparo et al. 2006; Song et al.
231 2011; Yamaguchi et al. 2011; Yumita et al. 2011). Studies regarding ALA and PpIX
232 mediated SDT have also provided encouraging results (Wang et al. 2010; Song et al.
233 2011; Li et al. 2012; Lv et al. 2012; Su et al. 2014), however, knowledge of ALA
234 mediated SDT for malignant gliomas is limited yet (Ohmura et al. 2011; Jeong et al.
235 2012).

236 Ultrasound exposure to biological tissues is categorized into two effects: thermal and
237 non-thermal. Acoustic energy absorbed by a biological tissue produces a temperature
238 elevation and the thermal effect is utilized for hyperthermia. But heat injury sometimes
239 causes crucial problem in treatment of intracranial lesions. Consequently, our concept of
240 this study is that the principle of SDT for brain tumor should be based on non-thermal

effect.

A non-thermal effect is caused by various mechanisms of mechanical and chemical phenomena. Acoustic radiation force produces tissue motion and acoustic streaming, which increase cell membrane permeability and resulting drug delivery efficiency. Cavitation is an important mechanism of the non-thermal effect and is categorized into non-inertial and inertial cavitation. Non-inertial cavitation is caused by microbubble oscillation under applied pressure and mainly produces mechanical effects, such as microstreaming, excess temperature elevation, and acoustic radiation force. Inertial cavitation occurs under a condition with higher intensity and longer duration than those in the non-inertial condition. Bubble expansion and subsequent rapid adiabatic contraction by inertia of the surrounding liquid causes a temperature rise inside the bubble up to several thousands of degrees, in theory, generating free radicals by pyrolysis of H_2O molecules. Generation of the free radicals is essential to induce SDT effects, a series of chemical reactions of a sonosensitizer such as porphyrin derivatives that was originally used as light activated chemicals. Porphyrin derivatives themselves have no anti-tumor effects, and are less cytotoxic for normal tissues; however, inertial

257 cavitation can be followed by energy transfer to oxygen to generate ROS in the
258 presence of porphyrin derivatives, (Canaparo et al. 2006) and they are expected to
259 provide an anti-tumor effect without temperature rising.
260 Apoptosis is suggested as the mechanism of cell death by PDT. Apoptosis can be
261 induced by low intensity ultrasound exposure even below the threshold for temperature
262 elevation of the culture medium (Lagneaux et al. 2002; Feng et al. 2010; Cheng et al.
263 2013). In addition, Zhang et al. showed that low intensity ultrasound exposure can
264 induce apoptosis related to caspase-3, Bcl-2, and survivin in C6 cells (Zhang et al.
265 2012). In our study, flow cytometry analysis confirmed that ultrasound exposure
266 induced cell apoptosis at 0.16 W/cm^2, even in the absence of a sonosensitizer. On the
267 other hand, cell survival analysis using immunofluorescences did not indicate the
268 presence of apoptosis in the ultrasound alone group. This discrepancy may be caused by
269 tumor-doubling time because measurement was performed 24 hours after treatment.
270 However, an important consideration is that survival rate of SDT group is still
271 suppressed. The sonication conditions are not fully determined, although they may have
272 been well reproduced between experiments, and will require further research.

Our findings also demonstrated a relationship between sonodynamic efficacy and the relative fluorescence intensity of sonosensitizer per cell, referring to the degree of intracellular accumulation of sonosensitizer per cell. We confirmed that the cytotoxicity of SDT was distinct between C6 and U87MG cells, and the efficacy of SDT could depend on the degree of intracellular accumulation of sonosensitizer for each cell line. Yumita et al. also reported that the efficacy of SDT closely correlate with the concentration of sonosensitizer in medium (Yumita et al. 2010). Moreover, results of clinical research showed that PpIX accumulates in tumor cells in a histopathological grade-specific manner after administration of ALA for intraoperative fluorescence diagnosis of malignant gliomas (Ishizuka et al. 2011). This data may support that the peak of the fluorescence intensity of the photo-/sonosensitizer is distinct among different cell lines. Therefore, therapeutic strategies to avoid the regulatory feedback in heme biosynthesis for accumulation of PpIX in tumor cells should be considered to obtain an efficient anti-tumor effect of ALA mediated SDT. For example, Xu et al. reported the efficacy of SDT for the glioma stem-like cells was improved by the inhibition of ATP-binding cassette sub-family G member 2 (ABCG2) transporter

289 function, which regulates cellular accumulation of porphyrin derivatives, with a specific
290 inhibitor (Xu et al. 2013).

291 When considering the development of SDT as clinical application, if the sonication
292 could be given through the skull, SDT will be an ideal noninvasive treatment for
293 malignant brain tumors. This may be possible in the near future given the research
294 conducted nowadays on brain ultrasound imaging and therapy. Because magnetic
295 resonance imaging guided focused ultrasound surgery (ExAblate® Neuro; InSightec,
296 Haifa, Israel) has already been applied in global clinical trial to treat neurological
297 disorders. This device induces focused tissue coagulation via ultrasound exposure
298 generating the thermal effect through intact skull, which has been attracted as an
299 alternative to deep brain stimulation (Lipsman et al. 2014). Clinical trials for
300 transcranial focal ablation of deep-seated tumors, especially glioblastoma, have started
301 (Ram et al. 2006; McDannold et al. 2010). However, there might be a limit to control
302 infiltrative tumor cells by "thermal" effect when considering the injurious effect upon
303 adjacent normal brain tissues. Hence, SDT based on "non-thermal" effect should be
304 established for treatment of deep-seated brain tumors.

CONCLUSIONS

In this study, SDT with porphyrin derivatives such as ALA, PpIX, and TS demonstrated the cytotoxic effect on glioma cells via apoptosis. Although further investigation will be necessary, the “non-thermal” SDT has the potential to be a new therapeutic modality for malignant gliomas.

311 **ACKNOWLEDGEMENTS**

312 This work was supported by Japan Society for the Promotion of Science (JSPS)

313 KAKENHI Grant Number 26670632. The authors thank Mr. Daiki Sekine at Laboratory

314 of Biological Engineering, Graduate School of Information Science and Technology,

315 Hokkaido University, and Ms. Yumiko Shinohe and Rika Nagashima at Department of

316 Neurosurgery, Graduate School of Medicine, Hokkaido University for their excellent

317 technical supports.

REFERENCES

Canaparo R, Serpe L, Catalano MG, Bosco O, Zara GP, Berta L, Frairia R. High energy shock waves (HESW) for sonodynamic therapy: effects on HT-29 human colon cancer cells. Anticancer Res 2006;26:3337-3342.

Chen H, Zhou X, Gao Y, Zheng B, Tang F, Huang J. Recent progress in development of new sonosensitizers for sonodynamic cancer therapy. Drug Discov Today 2014;19:502-509.

Cheng J, Sun X, Guo S, Cao W, Chen H, Jin Y, Li B, Li Q, Wang H, Wang Z, Zhou Q, Wang P, Zhang Z, Cao W, Tian Y. Effects of 5-aminolevulinic acid-mediated sonodynamic therapy on macrophages. Int J Nanomedicine 2013;8:669-676.

Chinot OL, Wick W, Mason W, Henriksson R, Saran F, Nishikawa R, Carpentier AF, Hoang-Xuan K, Kavan P, Cernea D, Brandes AA, Hilton M, Abrey L, Cloughesy T. Bevacizumab plus radiotherapy-temozolomide for newly diagnosed glioblastoma. N Engl J Med 2014;370:709-722.

Feng Y, Tian Z, Wan M. Bioeffects of low-intensity ultrasound in vitro: apoptosis, protein profile alteration, and potential molecular mechanism. J Ultrasound Med

2010;29:963-974.

Gilbert MR, Dignam JJ, Armstrong TS, Wefel JS, Blumenthal DT, Vogelbaum MA, Colman H, Chakravarti A, Pugh S, Won M, Jeraj R, Brown PD, Jaeckle KA, Schiff D, Stieber VW, Brachman DG, Werner-Wasik M, Tremont-Lukats IW, Sulman EP, Aldape KD, Curran WJ, Jr., Mehta MP. A randomized trial of bevacizumab for newly diagnosed glioblastoma. N Eng J Med 2014;370:699-708.

Ishizuka M, Abe F, Sano Y, Takahashi K, Inoue K, Nakajima M, Kohda T, Komatsu N, Ogura S, Tanaka T. Novel development of 5-aminolevurinic acid (ALA) in cancer diagnoses and therapy. Int Immunopharmacol 2011;11:358-365.

Jeong EJ, Seo SJ, Ahn YJ, Choi KH, Kim KH, Kim JK. Sonodynamically induced antitumor effects of 5-aminolevulinic acid and fractionated ultrasound irradiation in an orthotopic rat glioma model. Ultrasound Med Biol 2012;38:2143-2150.

Lagneaux L, de Meulenaer EC, Delforge A, Dejeneffe M, Massy M, Moerman C, Hannecart B, Canivet Y, Lepeltier MF, Bron D. Ultrasonic low-energy treatment: a novel approach to induce apoptosis in human leukemic cells. Exp Hematol 2002;30:1293-1301.

350 Li Y, Wang P, Zhao P, Zhu S, Wang X, Liu Q. Apoptosis induced by sonodynamic
351 treatment by protoporphyrin IX on MDA-MB-231 cells. Ultrasonics
352 2012;52:490-496.
353 Lipsman N, Mainprize TG, Schwartz ML, Hynynen K, Lozano AM. Intracranial
354 applications of magnetic resonance-guided focused ultrasound. Neurotherapeutics
355 2014;11:593-605.
356 Lv Y, Fang M, Zheng J, Yang B, Li H, Xiuzigao Z, Song W, Chen Y, Cao W.
357 Low-intensity ultrasound combined with 5-aminolevulinic acid administration in the
358 treatment of human tongue squamous carcinoma. Cell Physiol Biochem
359 2012;30:321-333.
360 McDannold N, Clement GT, Black P, Jolesz F, Hynynen K. Transcranial magnetic
361 resonance imaging- guided focused ultrasound surgery of brain tumors: initial
362 findings in 3 patients. Neurosurgery 2010;66:323-332.
363 Miyatake S, Kawabata S, Hiramatsu R, Furuse M, Kuroiwa T, Suzuki M. Boron neutron
364 capture therapy with bevacizumab may prolong the survival of recurrent malignant
365 glioma patients: four cases. Radiat Oncol 2014;9:6.

366 Muragaki Y, Akimoto J, Maruyama T, Iseki H, Ikuta S, Nitta M, Maebayashi K, Saito T,
367 Okada Y, Kaneko S, Matsumura A, Kuroiwa T, Karasawa K, Nakazato Y, Kayama T.
368 Phase II clinical study on intraoperative photodynamic therapy with talaporfin
369 sodium and semiconductor laser in patients with malignant brain tumors. J
370 Neurosurg 2013;119:845-852.
371 Nakamura H, Makino K, Yano S, Kuratsu J, Kumamoto Brain Tumor Research G.
372 Epidemiological study of primary intracranial tumors: a regional survey in
373 Kumamoto prefecture in southern Japan--20-year study. Int J Clin Oncol
374 2011;16:314-321.
375 Ohmura T, Fukushima T, Shibaguchi H, Yoshizawa S, Inoue T, Kuroki M, Sasaki K,
376 Umemura S. Sonodynamic therapy with 5-aminolevulinic acid and focused
377 ultrasound for deep-seated intracranial glioma in rat. Anticancer Res
378 2011;31:2527-2533.
379 Report of Brain Tumor Registry of Japan (2001-2004). Neurol Med Chir (Tokyo)
380 2014;54 Suppl 1:1-102.
381 Ram Z, Cohen ZR, Harnof S, Tal S, Faibel M, Nass D, Maier SE, Hadani M, Mardor Y.

382 Magnetic resonance imaging-guided, high-intensity focused ultrasound for brain
383 tumor therapy. Neurosurgery 2006;59:949-955.
384 Rosenthal I, Sostaric JZ, Riesz P. Sonodynamic therapy--a review of the synergistic
385 effects of drugs and ultrasound. Ultrason Sonochem 2004;11:349-363.
386 Song W, Cui H, Zhang R, Zheng J, Cao W. Apoptosis of SAS cells induced by
387 sonodynamic therapy using 5-aminolevulinic acid sonosensitizer. Anticancer Res
388 2011;31:39-45.
389 Stylli SS, Kaye AH. Photodynamic therapy of cerebral glioma--a review Part I--a
390 biological basis. J Clin Neurosci 2006a;13:615-625.
391 Stylli SS, Kaye AH. Photodynamic therapy of cerebral glioma - a review. Part II –
392 clinical studies. J Clin Neurosci 2006b;13:709-717.
393 Su X, Li Y, Wang P, Wang X, Liu Q. Protoporphyrin IX-mediated sonodynamic action
394 induces apoptosis of K562 cells. Ultrasonics 2014;54:275-284.
395 Thomas AA, Brennan CW, DeAngelis LM, Omuro AM. Emerging therapies for
396 glioblastoma. JAMA neurol 2014;71:1437-1444.
397 Wang X, Wang P, Tong W, Liu Q. Comparison of pharmacokinetics, intracellular

localizations and sonodynamic efficacy of endogenous and exogenous protoporphyrin IX in sarcoma 180 cells. Ultrasonics 2010;50:803-810.

Wilson CB. Glioblastoma: the past, the present, and the future. Clin Neurosurg 1992;38:32-48.

Xu ZY, Wang K, Li XQ, Chen S, Deng JM, Cheng Y, Wang ZG. The ABCG2 transporter is a key molecular determinant of the efficacy of sonodynamic therapy with Photofrin in glioma stem-like cells. Ultrasonics 2013;53:232-238.

Yamaguchi S, Kobayashi H, Narita T, Kanehira K, Sonezaki S, Kudo N, Kubota Y, Terasaka S, Houkin K. Sonodynamic therapy using water-dispersed TiO2-polyethylene glycol compound on glioma cells: comparison of cytotoxic mechanism with photodynamic therapy. Ultrason Sonochem 2011;18:1197-1204.

Yumita N, Han QS, Kitazumi I, Umemura S. Sonodynamically-induced apoptosis, necrosis, and active oxygen generation by mono-l-aspartyl chlorin e6. Cancer Sci 2008;99:166-172.

Yumita N, Iwase Y, Nishi K, Ikeda T, Komatsu H, Fukai T, Onodera K, Nishi H, Takeda K, Umemura S, Okudaira K, Momose Y. Sonodynamically-induced antitumor effect

414 of mono-l-aspartyl chlorin e6 (NPe6). Anticancer Res 2011;31:501-506.

415 Yumita N, Okudaira K, Momose Y, Umemura S. Sonodynamically induced apoptosis

416 and active oxygen generation by gallium-porphyrin complex, ATX-70. Cancer

417 Chemother Pharmacol 2010;66:1071-1078.

418 Zhang Z, Chen J, Chen L, Yang X, Zhong H, Qi X, Bi Y, Xu K. Low frequency and

419 intensity ultrasound induces apoptosis of brain glioma in rats mediated by caspase-3,

420 Bcl-2, and survivin. Brain Res 2012;1473:25-34.

421

422

423 **FIGURE LEGENDS**

424 Figure 1

425 Schematic diagram of experimental ultrasound irradiation apparatus set up.

426

427 Figure 2

428 Calcein AM (upper line), Ethidium homodimer (EthD-1) (middle line), and Hoechst
429 33342 (lower line) were stained on C6 cells 24 hours after treatment. Control represents
430 cells without any treatments, 5-Aminolevulinic acid (ALA) alone represents cells
431 cultured with 200 μg/mL of ALA for 4 hours, Ultrasound (US) alone represents cells
432 treated only with ultrasound at 1.0 MHz and 0.16 W/cm^2 for 60 seconds, and
433 Sonodynamic therapy (SDT) represents cells treated by ultrasound as described above
434 in the presence of 200 μg/mL of ALA. A significant number of exfoliated cells were
435 observed in the SDT group.

436

437 *Figure* 3

438 Survival rates of C6 cells and U87MG cells after treatment (a, d: 5-Aminolevulinic
439 acid (ALA) mediated sonodynamic therapy (SDT), b, e: Protoporphyrin IX (PpIX)
440 mediated SDT, c, f: Talaporfin sodium (TS) mediated SDT, upper line: C6 cells, lower
441 line: U87MG cells, n=3). Data are presented as the mean ± standard deviation and
442 statistical analysis was performed using one-way analyzed of variance (ANOVA)
443 followed by the Tukey-Kramer test. * shows a significant difference ($p<0.05$) between
444 groups. ALA alone; cells cultured with 200 μg/mL of ALA for 4 hours, PpIX alone;
445 cells cultured with 1.0 μg/mL of PpIX for 4 hours, TS alone; cells cultured with 30
446 μg/mL of TS for 4 hours, Ultrasound (US) alone; cells treated only with ultrasound at
447 1.0 MHz and 0.16 W/cm^2 for 60 seconds, and SDT; cells treated by US as described
448 above in the presence of each sonosensitizer.
449
450 Figure 4
451 Apoptosis and necrosis rates on C6 cells were analyzed via flow cytometry with
452 Annexin V and Propidium iodide (PI) costaining to assess the mechanism of cell
453 damage in 5-Aminolevulinic acid (ALA) mediated sonodynamic therapy (SDT) (a:

454 control group, b: ALA alone group, c: ultrasound alone group, d: SDT group). The
455 results were interpreted in the following fashion: cells in the lower-left quadrant
456 (Annexin-V-/PI-) represent living cells, those in the lower-right quadrant
457 (Annexin-V+/PI-) represent early apoptotic cells, and those in the upper-right quadrant
458 (Annexin-V+/PI+) represent late apoptotic or necrotic cells.
459
460 Figure 5
461 Relative fluorescence intensities of accumulated sonosensitizer in C6 and U87MG
462 cells were analyzed via flow cytometry. For each sonosensitizer, the fluorescence
463 intensity per cell of the U87MG cells was lower than that of the C6 cells. (a, d:
464 5-Aminolevulinic acid (ALA), b, e: Protoporphyrin IX (PpIX), c, f: Talaporfin sodium
465 (TS), upper line: C6 cells, lower line: U87MG cells)

Figure 1

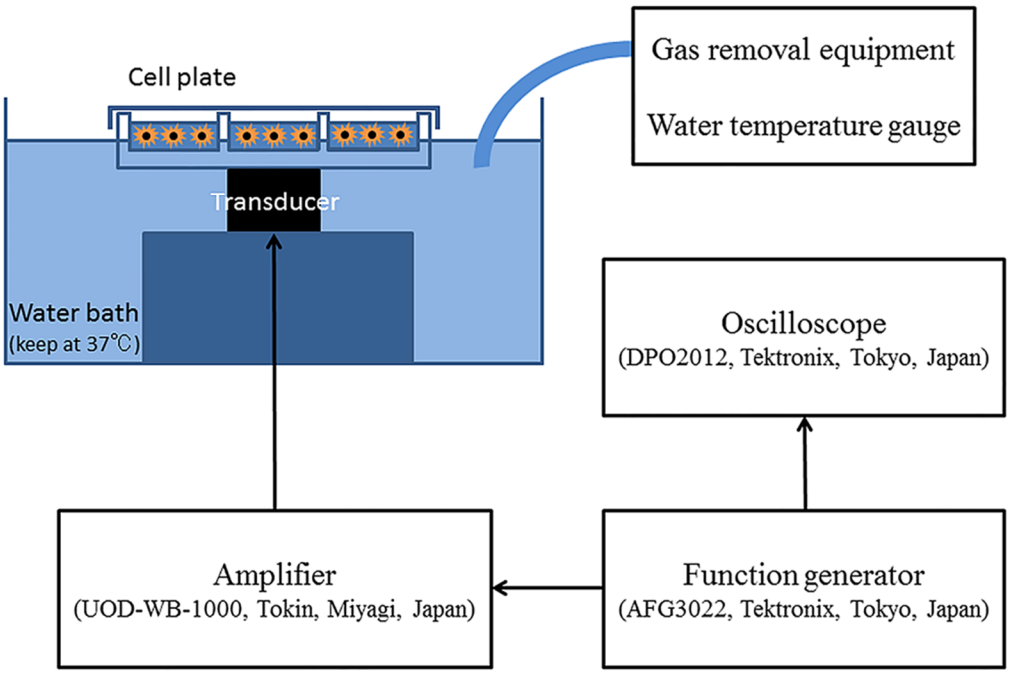
Gas removal equipment
Water temperature gauge
Cell plate
Transducer
Water bath
(keep at 37℃)
Oscilloscope
(DPO2012, Tektronix, Tokyo, Japan)
Amplifier
(UOD-WB-1000, Tokin, Miyagi, Japan)
Function generator
(AFG3022, Tektronix, Tokyo, Japan)

Figure 2

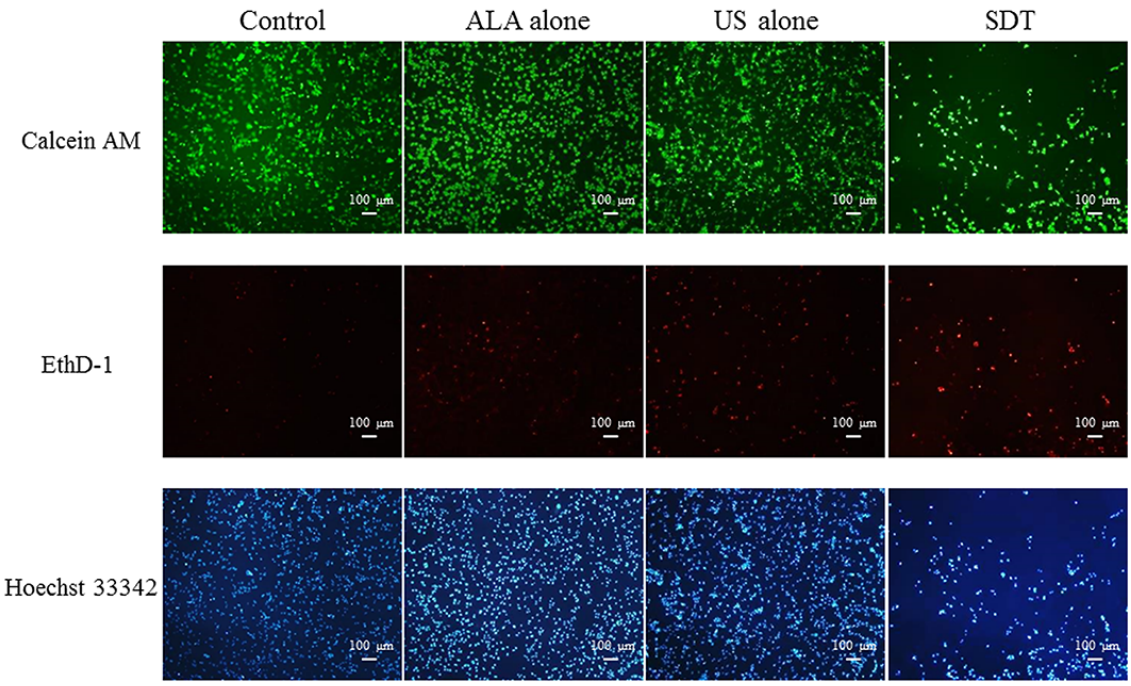
Control
ALA alone
US alone
SDT
Calcein AM
EthD-1
Hoechst 33342
100 μm

Figure 3

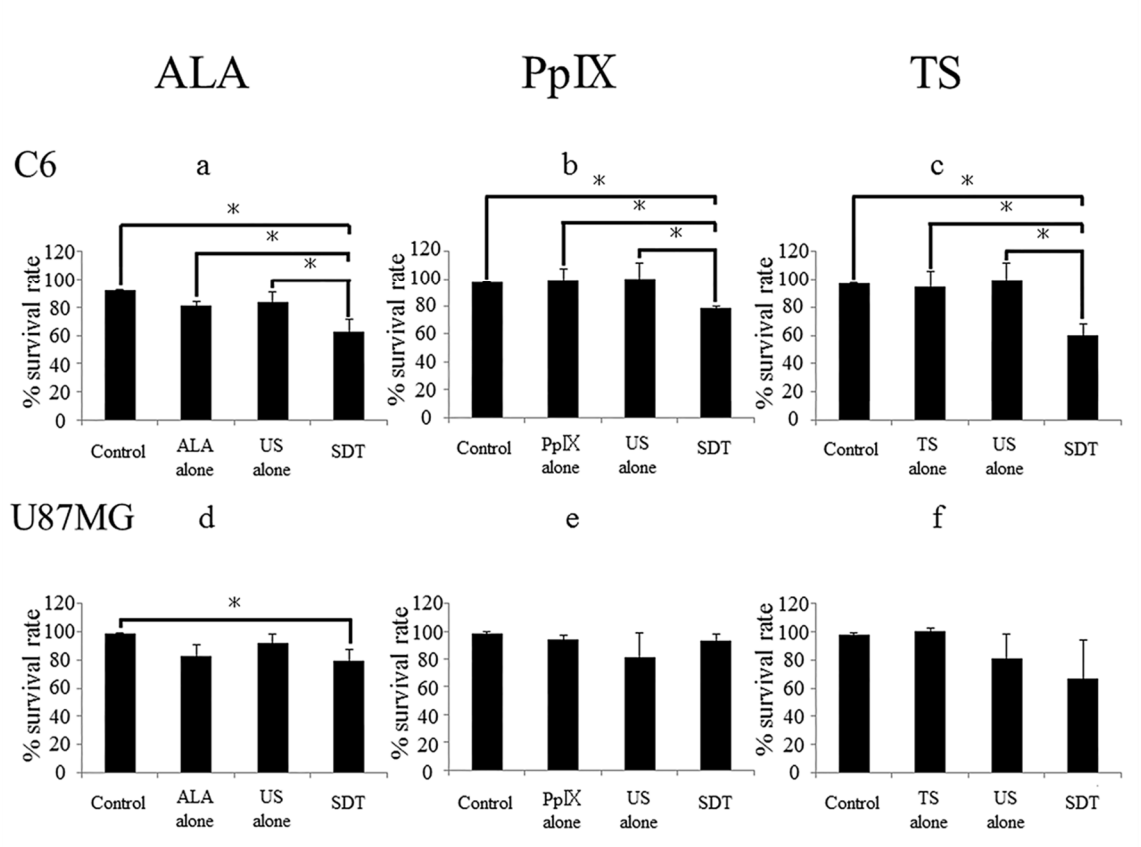
ALA
PpIX
TS
C6
a
b
c
U87MG
d
e
f
% survival rate
0
20
40
60
80
100
120
Control
ALA alone
US alone
SDT
PpIX alone
TS alone
*

Figure 4

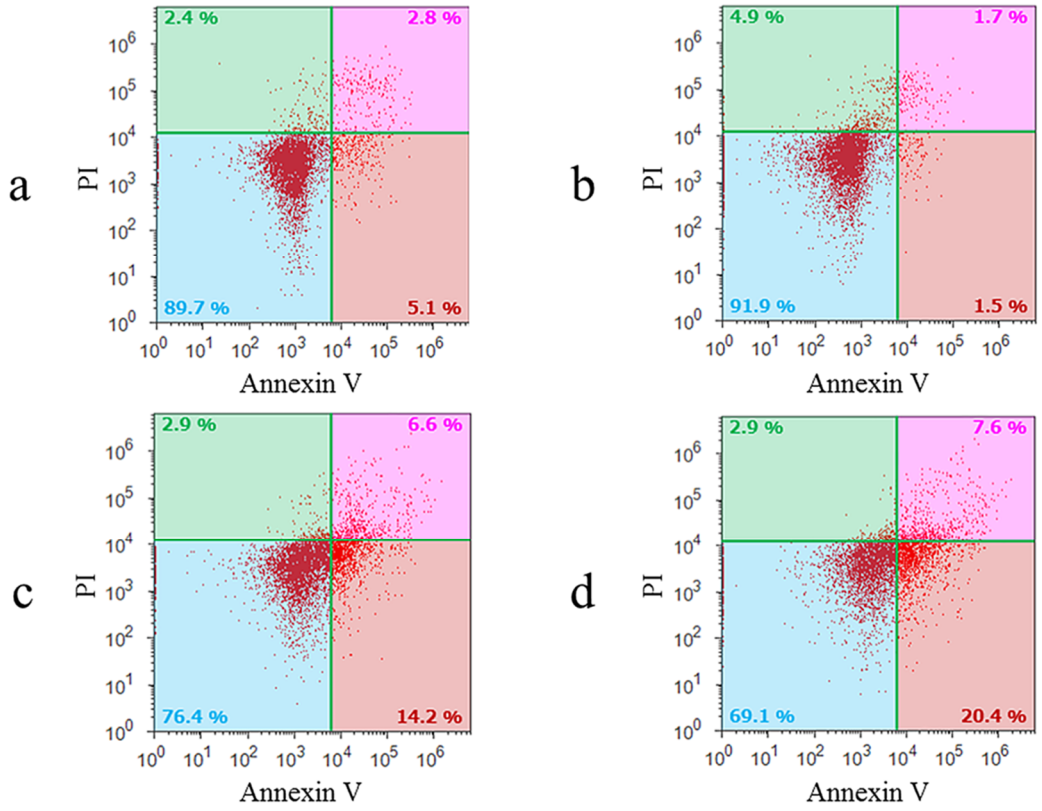
a
2.4 %
2.8 %
89.7 %
5.1 %
PI
Annexin V
b
4.9 %
1.7 %
91.9 %
1.5 %
PI
Annexin V
c
2.9 %
6.6 %
76.4 %
14.2 %
PI
Annexin V
d
2.9 %
7.6 %
69.1 %
20.4 %
PI
Annexin V

Figure 5

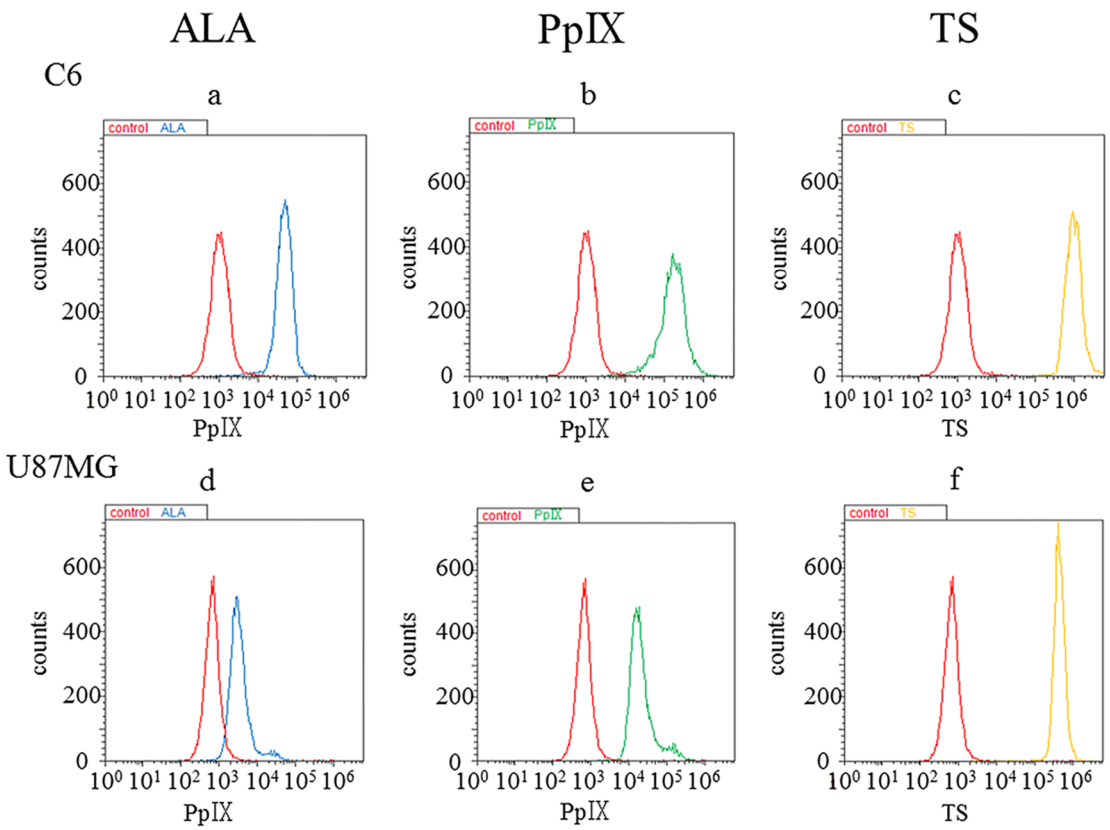
ALA
PpIX
TS
C6
a
b
c
control ALA
control PpIX
control TS
counts
PpIX
TS
U87MG
d
e
f